

Research Article

Spectral Unmixing Imaging for Differentiating Brown Adipose Tissue Mass and Its Activation

Jing Yang,^{1,2} Jian Yang,^{1,3} and Chongzhao Ran ¹

¹Molecular Imaging Laboratory, MGH/MIT/HMS Athinoula A. Martinos Center for Biomedical Imaging, Department of Radiology, Massachusetts General Hospital/Harvard Medical School, Room 2301, Building 149, Charlestown, Boston, MA 02129, USA

²School of Pharmacy, Soochow University, Suzhou 215006, China

³Center for Drug Discovery, School of Pharmacy, China Pharmaceutical University, Nanjing 210009, China

Correspondence should be addressed to Chongzhao Ran; cran@nmr.mgh.harvard.edu

Received 30 August 2017; Revised 5 December 2017; Accepted 11 December 2017; Published 4 January 2018

Academic Editor: Giancarlo Pascali

Copyright © 2018 Jing Yang et al. This is an open access article distributed under the Creative Commons Attribution License, which permits unrestricted use, distribution, and reproduction in any medium, provided the original work is properly cited.

Recent large-scale clinical analysis indicates that brown adipose tissue (BAT) mass levels inversely correlate with body-mass index (BMI), suggesting that BAT is associated with metabolic disorders such as obesity and diabetes. PET imaging with 18F-FDG is the most commonly used method for visualizing BAT. However, this method is not able to differentiate between BAT mass and BAT activation. This task, in fact, presents a tremendous challenge with no currently existing methods to separate BAT mass and BAT activation. Our previous results indicated that BAT could be successfully imaged in mice with near infrared fluorescent (NIRF) curcumin analogues. However, the results from conventional NIRF imaging could not reflect what portion of the NIRF signal from BAT activation contributed to the signal observed. To solve this problem, we used spectral unmixing to separate/unmix NIRF signal from oil droplets in BAT, which represents its mass and NIRF signal from blood, which represents BAT activation. In this report, results from our proof-of-concept investigation demonstrated that spectral unmixing could be used to separate NIRF signal from BAT mass and BAT activation.

1. Introduction

Brown adipose tissue (BAT) has been considered as “good fat,” due to its function of dissipating large amounts of chemical/food energy as heat to maintain the energy balance of the whole body [1–3]. Investigations of BAT have been ongoing for decades, particularly using animals. Reportedly, BAT has been assumed to have no physiologic relevance in adult humans, even though it is highly abundant in embryonic and early postnatal stages. However, this dogmatic opinion has been overturned by large clinical studies. In 2009, Cypess et al. reported that, by analyzing 3640 PET-CT images of 1,972 patients, BMI (body-mass index) inversely correlated with the amount of BAT, strongly suggesting that BAT is an important target in obesity and diabetes [4]. The existence of BAT in adults has been strongly endorsed by other important investigations as well [5–11]. Moreover, since 2009 numerous groundbreaking studies strongly support the significance

and potential benefits of BAT [12–33]. Characteristically, BAT contains a large number of mitochondria, abundant uncoupling protein-1 (UCP-1) expression, numerous small oil droplets in a single cell, and significant vascularization of BAT tissue [4, 34–37]. The above characteristics strongly imply that BAT plays an important role in metabolism and energy expenditure; therefore BAT is a potential target for diabetes and obesity therapy.

The assumption that BAT is “nonexistent” in adults is partially due to the lack of proper imaging methods to “see” the small BAT depots *in vivo*, as only 3%–8% of adult patients’ BAT depots could be clearly visualized with 18F-FDG if no cold or drug stimulation is applied [38–40]. However, under stimulated conditions, PET-FDG imaging has shown that BAT is still present in 95% health adults in the upper chest, neck, and other locations [4, 6, 8, 34, 35]. This remarkably large difference between unstimulated and stimulated conditions strongly indicates that PET-FDG

imaging only reflects the activation of BAT, but not BAT mass. Therefore, imaging probes that can consistently report BAT mass are highly desirable.

Accurately reporting BAT mass is a tremendous challenge for imaging scientists, due to the fact that BAT mass and BAT activation are intertwined under various conditions. It is obvious that there is no absolute “resting” status of BAT, and BAT activation cannot be “zero” for a living subject. Therefore, dissection of BAT mass and BAT activation is a remarkable challenge. However, most of the current imaging methods often reflect the summed signal from BAT mass and activation. Although PET-FDG imaging has significantly contributed to the “rediscovery” of BAT in adults, it primarily reflects BAT activation, but not BAT mass [41]. Similarly, most of other reported imaging methods are also BAT activation dependent [24, 41–51]. Our group has recently reported that near infrared fluorescence (NIRF) probe CRANAD- X ($X = -2, -3, \text{ and } -29$) could be used for BAT mass imaging [52], and Cerenkov luminescence imaging with ^{18}F -FDG could be applied to image BAT in mice [53]. Via conventional NIRF imaging with CRANAD-29, BAT mass change in a streptozotocin-induced diabetic mouse model and BAT activation under cold exposure could be reported. In addition, the same method could be used to monitor “browning” of WAT that was induced by β_3 -adrenoceptor agonist CL316,243 [52]. However, conventional NIRF imaging is not capable of dissecting the signal from BAT mass and from BAT activation.

To the best of our knowledge, there is no available imaging method for differentiating BAT mass and activation. The key to this challenge is to dissect BAT mass measurement from BAT physiology status (activated or suppressed). It is well known that BAT is highly vascularized, and activation of BAT is tightly closely associated with a significant increase of blood flow. Therefore, the change of blood flow has been considered to be a biomarker for BAT activation [54–56]. For a hydrophobic NIRF probe, its emission spectra are highly dependent on its environments [57]. In a hydrophobic environment such as in oil droplet of BAT mass, its emission spectra would be significantly blue-shifted [57]. Therefore, for the same NIRF probe, there will be apparent difference between the spectra from oil droplets of BAT and the spectra from blood flow. Previously, we have successfully utilized spectral unmixing technique to differentiate bound and free probe in the case of in vivo amyloid beta detection [58]. In this report, we demonstrated that spectral unmixing could be used to dissect NIRF signal from BAT mass and NIRF signal from blood flow [59]. With this technique, it is feasible to accurately report BAT mass and BAT activation/physiological status.

2. Methods and Materials

The reagents used for the synthesis were purchased from Aldrich and used without further purification. CRANAD-29 was synthesized according to our previously reported procedures [52]. All animal experimental procedures were approved by the Institutional Animal Care and Use Committee (IACUC) at Massachusetts General Hospital and carried

out in accordance with the approved guidelines. *In vivo* NIRF imaging was performed using the IVIS[®] Spectrum animal imaging system (Caliper Life Sciences, Perkin Elmer, Hopkinton, MA), and data analysis was conducted using Living Image[®] 4.2.1 software. Mice were anesthetized with isoflurane balanced with oxygen during image acquisition (less than 5 minutes for each imaging session).

2.1. Ex Vivo Spectral Unmixing with Dissected BAT and Blood. A two-month-old balb/c mouse was injected intravenously with 100 μL CRANAD-29 (0.4 mg/kg, 15% DMSO, 15% Cremophor EL, and 70% PBS pH 7.4). The mouse was sacrificed at 4 hours after the injection. BAT was dissected and 0.1 mL blood was collected. Sequence images were acquired with the following parameters: Ex/Em pairs: 605/660 nm, 640/680 nm, 640/700, 640/720 nm, 675/740 nm, 675/760 nm, and 675/780 nm. Exposure time is auto, FOV = B. Spectral unmixing was performed with Living Image[®] 4.2.1 software, and manual unmixing method was selected. The generated spectra for autofluorescence, BAT, and blood were saved as a spectral library for CRANAD-29.

2.2. In Vivo Spectral Unmixing of CRANAD-29 in Mice. A two-month-old balb/c mouse was injected intravenously with 100 μL CRANAD-29 (0.4 mg/kg, 15% DMSO, 15% Cremophor EL, and 70% PBS pH 7.4) in a 25°C room. Sequence images were captured at 4 hours after CRANAD-29 injection with the following parameters: Ex/Em pairs: 605/660 nm, 640/680 nm, 640/700, 640/720 nm, 675/740 nm, 675/760 nm, and 675/780 nm. Exposure time is auto, FOV = D. Spectral unmixing was performed with Living Image[®] 4.2.1 software, and Library Unmixing Method was selected.

2.3. In Vivo Spectral Unmixing of CRANAD-29 in Mice under Short Cold Exposure. Two-month-old balb/c mice ($n = 5$) were placed in a 4°C cold room for 2 hours before intravenous injection of CRANAD-29. After CRANAD-29 was totally washed out (about 10 days because of the slow clearance of CRANAD-29), the same group of mice were used as the control group ($n = 5$) and were placed in a 25°C room. Sequence images were acquired at 4 hours after probe injection with the same parameters as above in vivo imaging. For the cold exposure group, the mice were maintained at 4°C for 4 hours after probe injection. Spectral unmixing was performed with Living Image[®] 4.2.1 software, and Library Unmixing Method was selected. ROIs were manually drawn around the BAT area.

3. Results and Discussions

In our previous report, with conventional NIRF imaging, we demonstrated that CRANAD-29 had significant selectivity for BAT over WAT and could be used to monitor BAT activation and BAT mass changes [52]. For a NIRF probe, its residing environments have significant impact on its fluorescence properties, including intensity, emission spectrum, and lifetime. We hypothesized that the emission spectra of the same NIRF probe were different from oil droplets in BAT mass and from blood flow, due to their different residing

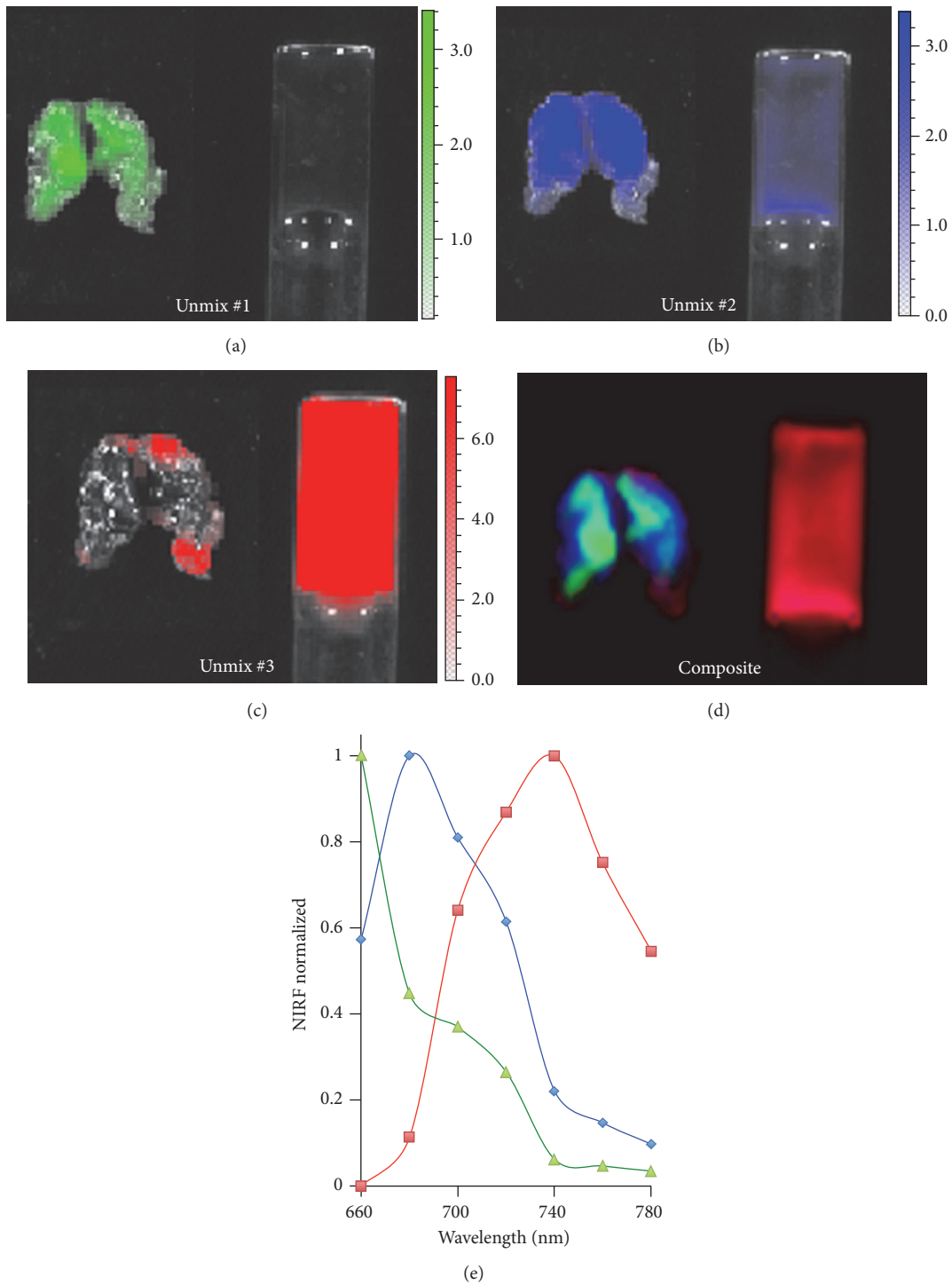


FIGURE 1: Spectral unmixing with CRANAD-29 for ex vivo BAT and blood. (a) Unmixed #1 represents autofluorescence signal and is corresponding to green line spectrum in (e). (b) Unmixed #1 represents NIRF signal from BAT mass and is corresponding to blue line spectrum in (e). (c) Unmixed #2 is for NIRF from blood and red line spectrum in (e). (d) Merged image of unmixed #1, #2, and #3. (e) Ex vivo unmixed spectra for autofluorescence (green), BAT mass (blue), and blood flow (red).

environments, and the spectral difference could be used for spectral unmixing.

To validate our hypothesis, we first conducted spectral unmixing imaging with ex vivo BAT tissue and blood from

a mouse injected with CRANAD-29. Sequence images were acquired with seven Ex/Em pairs, and spectral unmixing was conducted with Living Image® 4.2.1 software. As expected, we were able to differentiate BAT and blood, as evidenced

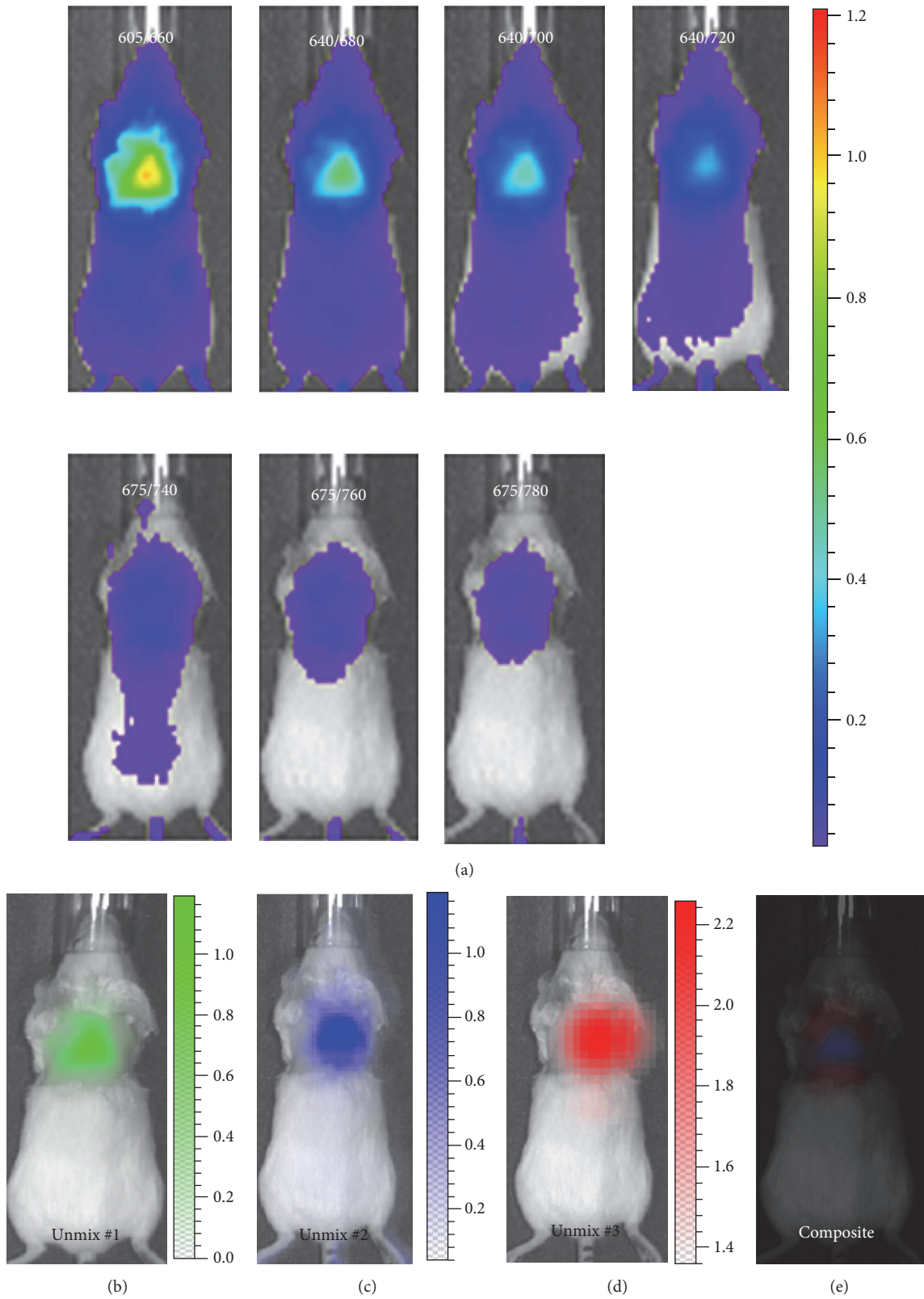


FIGURE 2: Spectral unmixing with CRANAD-29 in vivo imaging. (a) Raw images of CRANAD-29 before spectral unmixing. (b) Unmixed autofluorescence signal. (c) Unmixed NIRF signal from BAT mass. (d) Unmixed NIRF signal from blood flow. (e) Merged image of unmixed #2 and #3. Note: for clarity, unmixed #1 was not merged.

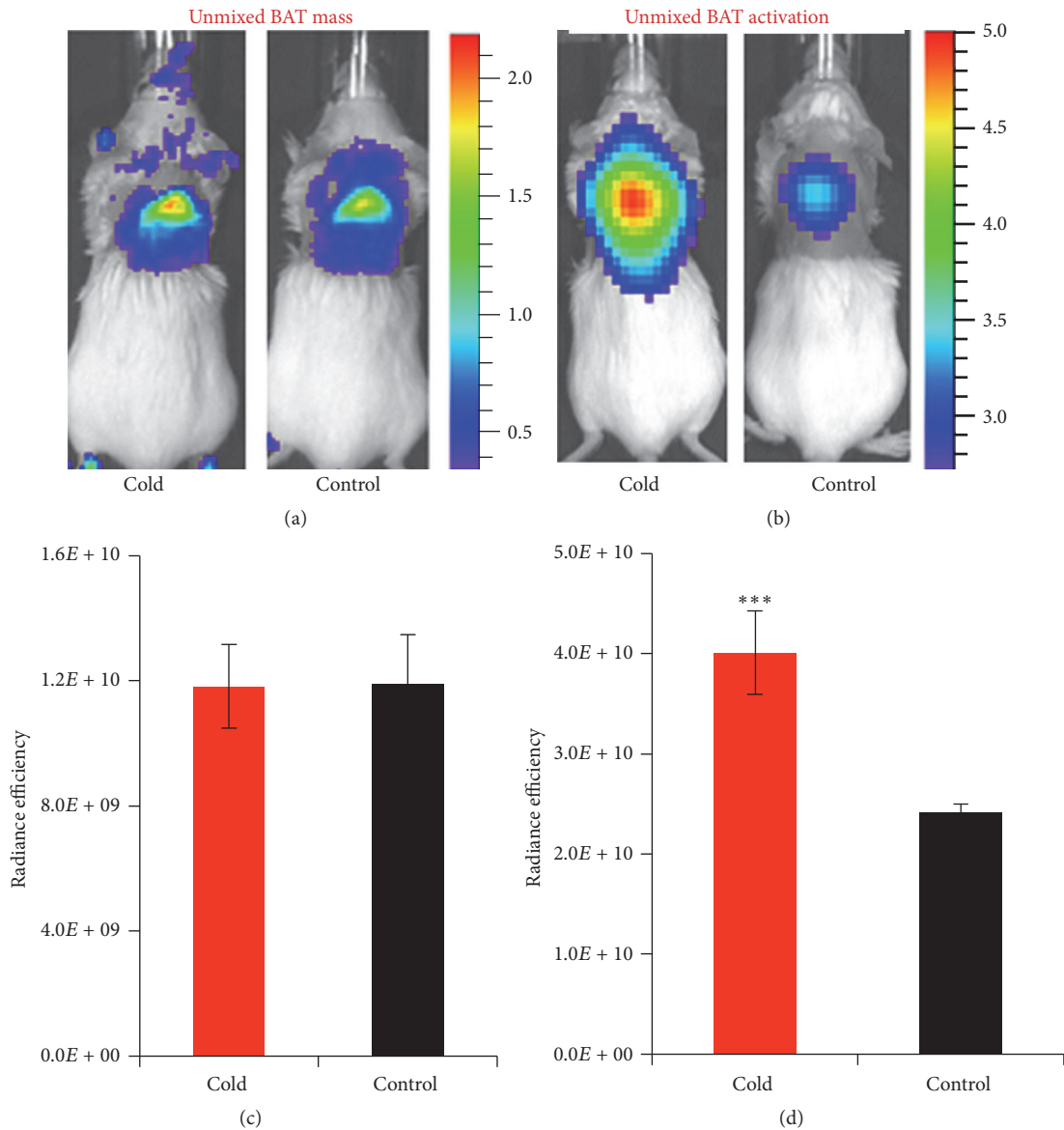


FIGURE 3: Spectral unmixing with CRANAD-29 for in vivo imaging under cold treatment. (a) Unmixed NIRF signal from BAT mass under cold treatment and control condition. (b) Unmixed NIRF signal from blood flow reflecting BAT activation. (c-d) Quantitative analysis of unmixed NIRF signal from BAT mass (c) and blood flow (d) under cold treatment and the control condition. *** $p < 0.005$.

by the well-separated images (Figures 1(a)–1(d)) and spectra from BAT and blood (Figure 1(e)). The spectra generated from this ex vivo unmixing were saved as a spectral library of CRANAD-29, which can be used for in vivo unmixing investigation.

To further validate the feasibility of spectral unmixing for in vivo studies, we acquired sequence images with the same parameters as the above ex vivo experiment with a mouse that was injected CRANAD-29. We used the spectral library of CRANAD-29 to conduct the spectral unmixing. As shown in Figure 2, the autofluorescence, signal of BAT, and blood stream could be well-separated, suggesting that the spectral unmixing is feasible for in vivo imaging.

To investigate spectral unmixing which could be used to dissect the signals from BAT mass and BAT activation, we conducted proof-of-concept experiment with the same group of mice with and without short cold exposure. The group of mice ($n = 5$) were treated with a short cold exposure (2 hours) and injected with CRANAD-29. After 4 hours of the injection. Sequence images were captured with the same parameters as above. After CRANAD-29 totally washing out, the same mice without the cold treatment were imaged again with the probe. We compared the unmixed NIRF signals from BAT and blood flow under cold treatment and without cold exposure. Obviously, with such a short cold exposure, the BAT mass would not change, but the blood flow was

expected to significantly increase under the cold treatment. Indeed, we found that there was no significant NIRF signal difference from BAT mass (Figures 3(a) and 3(c), $p = 0.975$), but an apparent increase of NIRF signal from blood flow from the cold exposure condition, and the increase was about 1.66-fold (Figures 3(b) and 3(d), $p = 0.005$). These results indicated that our method was reliable. Taken together, the above in vitro and in vivo data strongly indicated that spectral unmixing could be used to separate NIRF signal from BAT mass and BAT activation.

4. Conclusion

In this report, we developed a spectral unmixing method that could be, for the first time, to differentiate BAT mass and BAT activation. We believe that our method has the feasibility to reliably report BAT mass changes under different genetic manipulation and drug treatment in preclinical studies. Our cost-efficient NIRF imaging has a potential impact on pre-clinical animal studies and will greatly assist drug discovery and basic research related to BAT.

Conflicts of Interest

The authors declare that there are no conflicts of interest regarding the publication of this paper.

Acknowledgments

This work was supported by NIH/NIDDK R56DK108813 award (Chongzhao Ran). The authors also acknowledge China Scholarship Council of Ministry of Education of China for support (Jing Yang and Jian Yang).

References

- [1] B. Cannon and J. Nedergaard, "Brown adipose tissue: function and physiological significance," *Physiological Reviews*, vol. 84, no. 1, pp. 277–359, 2004.
- [2] D. Richard and F. Picard, "Brown fat biology and thermogenesis," *Frontiers in Bioscience: A Journal and Virtual Library*, vol. 16, no. 4, pp. 1233–1260, 2011.
- [3] V. Ouellet, S. M. Labbé, D. P. Blondin et al., "Brown adipose tissue oxidative metabolism contributes to energy expenditure during acute cold exposure in humans," *The Journal of Clinical Investigation*, vol. 122, no. 2, pp. 545–552, 2012.
- [4] A. M. Cypess, S. Lehman, G. Williams et al., "Identification and importance of brown adipose tissue in adult humans," *The New England Journal of Medicine*, vol. 360, no. 15, pp. 1509–1517, 2009.
- [5] B. P. Leitner, S. Huang, R. J. Brychta et al., "Mapping of human brown adipose tissue in lean and obese young men," *Proceedings of the National Academy of Sciences of the United States of America*, vol. 114, no. 32, pp. 8649–8654, 2017.
- [6] W. D. van Marken Lichtenbelt, J. W. Vanhommerig, N. M. Smulders et al., "Cold-activated brown adipose tissue in healthy men," *The New England Journal of Medicine*, vol. 360, no. 15, pp. 1500–1508, 2009.
- [7] F. S. Celi, "Brown adipose tissue - when it pays to be inefficient," *The New England Journal of Medicine*, vol. 360, no. 15, pp. 1553–1556, 2009.
- [8] K. A. Virtanen, M. E. Lidell, J. Orava et al., "Functional brown adipose tissue in healthy adults," *The New England Journal of Medicine*, vol. 360, no. 15, pp. 1518–1525, 2009.
- [9] T. Yoneshiro, S. Aita, M. Matsushita et al., "Age-related decrease in cold-activated brown adipose tissue and accumulation of body fat in healthy humans," *Obesity*, vol. 19, no. 9, pp. 1755–1760, 2011.
- [10] S. Enerbäck, "The origins of brown adipose tissue," *The New England Journal of Medicine*, vol. 360, no. 19, pp. 2021–2023, 2009.
- [11] S. R. Farmer, "Be cool, lose weight," *Nature*, vol. 458, no. 7240, pp. 839–840, 2009.
- [12] S. Kajimura, P. Seale, K. Kubota et al., "Initiation of myoblast to brown fat switch by a PRDM16-C/EBP- β transcriptional complex," *Nature*, vol. 460, no. 7259, pp. 1154–1158, 2009.
- [13] R. K. Gupta, Z. Arany, P. Seale et al., "Transcriptional control of preadipocyte determination by Zfp423," *Nature*, vol. 464, no. 7288, pp. 619–623, 2010.
- [14] P. Boström, J. Wu, M. P. Jedrychowski et al., "A PGC1- α -dependent myokine that drives brown-fat-like development of white fat and thermogenesis," *Nature*, vol. 481, no. 7382, pp. 463–468, 2012.
- [15] J. A. Timmons, K. Baar, P. K. Davidsen, and P. J. Atherton, "Is irisin a human exercise gene?" *Nature*, vol. 488, no. 7413, pp. E9–E10, 2012.
- [16] T. J. Schulz, P. Huang, T. L. Huang et al., "Brown-fat paucity due to impaired BMP signalling induces compensatory browning of white fat," *Nature*, vol. 495, no. 7441, pp. 379–383, 2013.
- [17] H. Ohno, K. Shinoda, K. Ohyama, L. Z. Sharp, and S. Kajimura, "EHMT1 controls brown adipose cell fate and thermogenesis through the PRDM16 complex," *Nature*, vol. 504, no. 7478, pp. 163–167, 2013.
- [18] T. Gnad, S. Scheibler, I. von Kügelgen et al., "Adenosine activates brown adipose tissue and recruits beige adipocytes via A_{2A} receptors," *Nature*, vol. 516, no. 7531, pp. 395–399, 2014.
- [19] M. Harms and P. Seale, "Brown and beige fat: development, function and therapeutic potential," *Nature Medicine*, vol. 19, no. 10, pp. 1252–1263, 2013.
- [20] Q. A. Wang, C. Tao, R. K. Gupta, and P. E. Scherer, "Tracking adipogenesis during white adipose tissue development, expansion and regeneration," *Nature Medicine*, vol. 19, no. 10, pp. 1338–1344, 2013.
- [21] A. M. Cypess, A. P. White, C. Vernochet et al., "Anatomical localization, gene expression profiling and functional characterization of adult human neck brown fat," *Nature Medicine*, vol. 19, no. 5, pp. 635–639, 2013.
- [22] M. E. Lidell, M. J. Betz, O. D. Leinhard et al., "Evidence for two types of brown adipose tissue in humans," *Nature Medicine*, vol. 19, no. 5, pp. 631–634, 2013.
- [23] K. J. Williams and E. A. Fisher, "Globular warming: how fat gets to the furnace," *Nature Medicine*, vol. 17, no. 2, pp. 157–159, 2011.
- [24] A. Bartelt, O. T. Bruns, R. Reimer et al., "Brown adipose tissue activity controls triglyceride clearance," *Nature Medicine*, vol. 17, no. 2, pp. 200–205, 2011.
- [25] B. Cannon and J. Nedergaard, "Thyroid hormones: igniting brown fat via the brain," *Nature Medicine*, vol. 16, no. 9, pp. 965–967, 2010.
- [26] Y. Qiu, K. D. Nguyen, J. I. Odegaard et al., "Eosinophils and type 2 cytokine signaling in macrophages orchestrate development of functional beige fat," *Cell*, vol. 157, no. 6, pp. 1292–1308, 2014.

- [27] R. R. Rao, J. Long, J. White et al., "Meteorin-like is a hormone that regulates immune-adipose interactions to increase beige fat thermogenesis," *Cell*, vol. 157, no. 6, pp. 1279–1291, 2014.
- [28] A. Fedorenko, P. V. Lishko, and Y. Kirichok, "Mechanism of fatty-acid-dependent UCP1 uncoupling in brown fat mitochondria," *Cell*, vol. 151, no. 2, pp. 400–413, 2012.
- [29] R. Teperino, S. Amann, M. Bayer et al., "Hedgehog partial agonism drives warburg-like metabolism in muscle and brown fat," *Cell*, vol. 151, no. 2, pp. 414–426, 2012.
- [30] L. Qiang, L. Wang, N. Kon et al., "Brown remodeling of white adipose tissue by SirT1-dependent deacetylation of Ppar γ ," *Cell*, vol. 150, no. 3, pp. 620–632, 2012.
- [31] J. Wu, P. Boström, L. M. Sparks et al., "Beige adipocytes are a distinct type of thermogenic fat cell in mouse and human," *Cell*, vol. 150, no. 2, pp. 366–376, 2012.
- [32] A. J. Whittle, S. Carobbio, L. Martins et al., "BMP8B increases brown adipose tissue thermogenesis through both central and peripheral actions," *Cell*, vol. 149, no. 4, pp. 871–885, 2012.
- [33] M. Yudasaka, Y. Yomogida, M. Zhang et al., "Near-infrared photoluminescent carbon nanotubes for imaging of brown fat," *Scientific Reports*, vol. 7, Article ID 44760, 2017.
- [34] J. Nedergaard, T. Bengtsson, and B. Cannon, "Unexpected evidence for active brown adipose tissue in adult humans," *American Journal of Physiology-Renal Physiology*, vol. 293, no. 2, pp. E444–E452, 2007.
- [35] T. T. Tran and C. R. Kahn, "Transplantation of adipose tissue and stem cells: role in metabolism and disease," *Nature Reviews Endocrinology*, vol. 6, no. 4, pp. 195–213, 2010.
- [36] Y.-H. Tseng, E. Kokkotou, T. J. Schulz et al., "New role of bone morphogenetic protein 7 in brown adipogenesis and energy expenditure," *Nature*, vol. 454, no. 7207, pp. 1000–1004, 2008.
- [37] H. Zhang, T. J. Schulz, D. O. Espinoza et al., "Cross talk between insulin and bone morphogenetic protein signaling systems in brown adipogenesis," *Molecular and Cellular Biology*, vol. 30, no. 17, pp. 4224–4233, 2010.
- [38] C. Cohade, K. A. Mourtzikos, and R. L. Wahl, "'USA-Fat': prevalence is related to ambient outdoor temperature-evaluation with 18F-FDG PET/CT," *Journal of Nuclear Medicine: Official Publication, Society of Nuclear Medicine*, vol. 44, no. 8, pp. 1267–1270, 2003.
- [39] P. Lee, K. K. Ho, and M. J. Fulham, "The importance of brown adipose tissue," *The New England Journal of Medicine*, pp. 419–420, 2009.
- [40] M. E. Lidell and S. Enerbäck, "Brown adipose tissue—a new role in humans?" *Nature Reviews Endocrinology*, vol. 6, no. 6, pp. 319–325, 2010.
- [41] A. M. Cypess, C. R. Haft, M. R. Laughlin, and H. H. Hu, "Brown fat in humans: consensus points and experimental guidelines," *Cell Metabolism*, vol. 20, no. 3, pp. 408–415, 2014.
- [42] A. Nakayama, A. C. Bianco, C.-Y. Zhang, B. B. Lowell, and J. V. Frangioni, "Quantification of brown adipose tissue perfusion in transgenic mice using near-infrared fluorescence imaging," *Molecular Imaging*, vol. 2, no. 1, pp. 37–49, 2003.
- [43] A. Azhdarinia, A. C. Daquinag, C. Tseng et al., "A peptide probe for targeted brown adipose tissue imaging," *Nature Communications*, vol. 4, article no. 2472, 2013.
- [44] D. R. Rice, A. G. White, W. M. Leevy, and B. D. Smith, "Fluorescence imaging of interscapular brown adipose tissue in living mice," *Journal of Materials Chemistry B: Materials for Biology and Medicine*, vol. 3, no. 9, pp. 1979–1989, 2015.
- [45] C. Wu, W. Cheng, H. Xing, Y. Dang, F. Li, and Z. Zhu, "Brown adipose tissue can be activated or inhibited within an hour before 18F-FDG injection: a preliminary study with micropet," *Journal of biomedicine & biotechnology*, Article ID 159834, p. 2011, 2011.
- [46] I. Madar, T. Isoda, P. Finley, J. Angle, and R. Wahl, "18F-fluorobenzyl triphenyl phosphonium: a noninvasive sensor of brown adipose tissue thermogenesis," *Journal of Nuclear Medicine*, vol. 52, no. 5, pp. 808–814, 2011.
- [47] H. H. Hu, D. L. Smith Jr, K. S. Nayak, M. I. Goran, and T. R. Nagy, "Identification of brown adipose tissue in mice with fat-water ideal-MRI," *Journal of Magnetic Resonance Imaging*, vol. 31, no. 5, pp. 1195–1202, 2010.
- [48] Y. I. Chen, A. M. Cypess, C. A. Sass et al., "Anatomical and functional assessment of brown adipose tissue by magnetic resonance imaging," *Obesity*, vol. 20, no. 7, pp. 1519–1526, 2012.
- [49] A. Khanna and R. T. Branca, "Detecting brown adipose tissue activity with bold MRI in mice," *Magnetic Resonance in Medicine*, vol. 68, no. 4, pp. 1285–1290, 2012.
- [50] X.-G. Peng, S. Ju, F. Fang et al., "Comparison of brown and white adipose tissue fat fractions in ob, seipin, and Fsp27 gene knockout mice by chemical shift-selective imaging and 1H-MR spectroscopy," *American Journal of Physiology-Endocrinology and Metabolism*, vol. 304, no. 2, pp. E160–E167, 2013.
- [51] R. T. Branca, T. He, L. Zhang et al., "Detection of brown adipose tissue and thermogenic activity in mice by hyperpolarized xenon MRI," *Proceedings of the National Academy of Sciences of the United States of America*, vol. 111, no. 50, pp. 18001–18006, 2014.
- [52] X. Zhang, Y. Tian, H. Zhang et al., "Curcumin analogues as selective fluorescence imaging probes for brown adipose tissue and monitoring browning," *Scientific Reports*, vol. 5, Article ID 13116, 2015.
- [53] X. Zhang, C. Kuo, A. Moore, and C. Ran, "In vivo optical imaging of interscapular brown adipose tissue with 18F-FDG via cerenkov luminescence imaging," *PLoS ONE*, vol. 8, no. 4, Article ID e62007, 2013.
- [54] O. Muzik, T. J. Mangner, and J. G. Granneman, "Assessment of oxidative metabolism in brown fat using PET imaging," *Frontiers in Endocrinology*, vol. 3, Article ID Article 15, 2012.
- [55] M. Clerte, D. M. Baron, P. Brouckaert et al., "Brown adipose tissue blood flow and mass in obesity: a contrast ultrasound study in mice," *Journal of the American Society of Echocardiography: Official Publication of The American Society of Echocardiography*, vol. 26, no. 12, pp. 1465–1473, 2013.
- [56] G. Abreu-Vieira, C. E. Hagberg, K. L. Spalding, B. Cannon, and J. Nedergaard, "Adrenergically stimulated blood flow in brown adipose tissue is not dependent on thermogenesis," *American Journal of Physiology-Endocrinology and Metabolism*, vol. 308, no. 9, pp. E822–E829, 2015.
- [57] J. R. Lakowicz, *Principles of Fluorescence Spectroscopy*, Plenum Publishing Corporation, 1999.
- [58] C. Ran and A. Moore, "Spectral unmixing imaging of wavelength-responsive fluorescent probes: an application for the real-time report of amyloid beta species in alzheimer's disease," *Molecular Imaging and Biology*, vol. 14, no. 3, pp. 293–300, 2012.
- [59] J. Yang, C. Qiao, A. Moore, and C. Ran, "Spectral unmixing imaging for differentiating brown adipose tissue mass and its activation," in *Proceedings of the World Molecular Imaging Congress*, New York, NY, USA, September 7–10, 2016.